Development of a Large Aperture Nb_3Sn Racetrack Quadrupole Magnet

Paolo Ferracin, Scott E. Bartlett, Shlomo Caspi, Daniel R. Dietderich, Steve A. Gourlay, Charles R. Hannaford, Aurelio R. Hafalia, Alan F. Lietzke, Sara Mattafirri, Alfred D. McInturff, Mark Nyman, Gianluca Sabbi

***Abstract*—The U.S. LHC Accelerator Research Program (LARP), a collaboration between BNL, FNAL, LBNL, and SLAC, has among its major objectives the development of advanced magnet technology for an LHC luminosity upgrade. The LBNL Superconducting Magnet Group supports this program with a broad effort involving design studies, Nb_3Sn conductor development, mechanical models, and basic prototypes. This paper describes the development of a large aperture Nb_3Sn racetrack quadrupole magnet using four racetrack coils from the LBNL Subscale Magnet (SM) Program. The magnet provides a gradient of 95 T/m in a 110 mm bore, with a peak field in the conductor of 11.2 T. The coils are pre-stressed by a mechanical structure based on a pre-tensioned aluminum shell, and axially supported with aluminum rods. The mechanical behavior has been monitored with strain gauges and the magnetic field has been measured. Results of the test are reported and analyzed.**

***Index Terms*—Superconducting magnet, Nb_3Sn, quadrupole magnet**

I. Introduction

FOUR US national laboratories (BNL, FNAL, LBNL, and SLAC) are currently engaged in the LHC Accelerator Research Program. One of the goals of the program is the development of magnets for the LHC Interaction Regions (IR) beyond the current design [1]–[3]. At the moment, the main objective consists of the design of a single bore Nb_3Sn quadrupole magnet [4].

In 2004, LBNL has been supporting the LARP effort with two experiments for technology development. The first experiment involves a mechanical structure for a cos(2ϑ) quadrupole magnet: the structure has been assembled around a dummy coil, instrumented with strain gauges, and measured at room temperature and at 77 K [5]. The second experiment involves a subscale quadrupole magnet (SQ01). The magnet implements Nb_3Sn racetrack coils designed for the LBNL Subscale Dipole Magnet Program [6]. In a subscale dipole magnet two coils are assembled in a common-coil (dipole) configuration, confined within an aluminum shell and pre-stressed with pressurized bladders [7]. In SQ01, four coils were arranged around a square bore plate in a quadrupole configuration. In the past, Nb_3Sn technology has been applied to pioneer quadrupole magnet models built at BNL [8] and at CERN [9]. Moreover, a racetrack coil design, but utilizing NbTi conductor, was adopted in quadrupole magnet prototypes for the Heavy Ion Fusion Program [10].

SQ01 is the first quadrupole magnet to implement the key and bladder technology. Its main goal was providing an early feedback, in realistic Lorentz force conditions, on a support structure similar to the one designed for the cos(2ϑ) quadrupole magnet. Setting reference values for coil stress and investigating Nb_3Sn low field instabilities in the parameter range of interest were also part of the objectives of this test. This paper reports magnet design and parameters, along with quench performance, strain gauge data and magnetic field measurements.

II. Magnetic Design

The design of the subscale quadrupole magnet (Fig. 1) consists of four subscale coil modules: SC01, SC02, SC15, and SC16. The first pair (old coils) was previously successfully tested in several subscale dipole magnets, while the second pair (new coils) was fabricated specifically for SQ01. The cables (see Table I) are composed of 20 Nb_3Sn strands with a diameter of 0.7 mm, and insulated with a 0.1 mm thick woven sleeve of fiberglass. The strands used in the cables of coil SC01 and SC02 were fabricated with the Modified Jelly Roll process [11], while the strands for the new coils were formed by the Restacked Rod Process [12].

Each coil module was wound around an iron pole (island) in a flat racetrack double-layer configuration and confined within a stainless steel horseshoe. After winding, the coils were reacted with the following heat treatment: 210 °C for 100 h, 340 °C for 48 h, and 650 °C for 180 h. The reaction time for coils SC15 and SC16 was shortened (650 °C for 72 h) to obtain a higher RRR value [13]. After reaction the coils were epoxy impregnated and placed around a square aluminum plate. The bore had a clear aperture of 110 mm and a square side of 128 mm (coil aperture).

Manuscript received October 5, 2004. This work was supported under Contract No. DE-AC03-76SF00098 by the Director, Office of Energy Research, Office of High Energy Physics, U.S. Department of Energy.

The authors are with the Lawrence Berkeley National Laboratory, Berkeley, CA 94720, USA (phone: +1-510-486-4630; fax: +1-510-486-4630; e-mail: pferracin@lbl.gov).

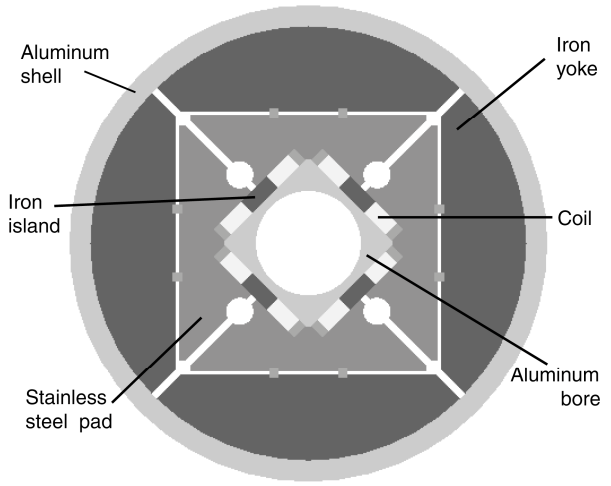

Fig. 1. SQ01 magnet cross-section

The main parameters of the magnet are listed in Table II. The peak field is located in the innermost turn of the end region, close to the island tip. The short sample value has been obtained by the intersection between the critical curves measured at LBNL on the two different strands and the computed magnet load line (Fig. 2). It can be noticed that a 5 % additional margin characterized the new coils with respect to the old ones.

TABLE I
CONDUCTOR PARAMETERS

	Units	SC01	SC02	SC15	SC16
Strand diameter	mm	0.7	0.7	0.7	0.7
Cu/Sc ratio		0.87	0.87	0.97	0.97
Manufacturer		OST	OST	OST	OST
Type		MJR	MJR	RRP	RRP
Jc @ 12 T/ 4.2 K	A/mm^2	2334	2334	3043	3043
RRR		38	37	99	87
Cable width	mm	7.938	7.938	7.884	7.884
Cable thickness	mm	1.280	1.280	1.267	1.267
No. strands		20	20	20	20
Insul. thickness	mm	0.1	0.1	0.1	0.1
No. turns		20	20	20	20

TABLE II
PERFORMANCE PARAMETERS

Parameter	Symbol	Unit	
Bore aperture	D_{bore}	mm	110
Coil aperture	D_{coil}	mm	128
Coil length (straight section)	l_{coil}	mm	150
Short sample gradient	G_{ss}	T/m	95
Short sample current	I_{ss}	kA	11.4
Coil peak field @ I_{ss}	B_{pk}	T	11.2
Inductance @ I_{ss}	L	mH	2.7
Stored energy @ I_{ss}	U	kJ	175
Axial Lorenz force per coil @ I_{ss}	F_z	kN	+ 95
Lorenz forces[a] in the straight section @ I_{ss}	F_x	N/mm	+ 720
	F_y	N/mm	- 922
	F_θ	N/mm	- 1161
	F_r	N/mm	- 143

[a] F_x and F_y are respectively the horizontal and vertical forces. F_θ and F_r are respectively the azimuthal (perpendicular to the wide side of the cable) and radial (parallel to the wide side of the cable) forces.

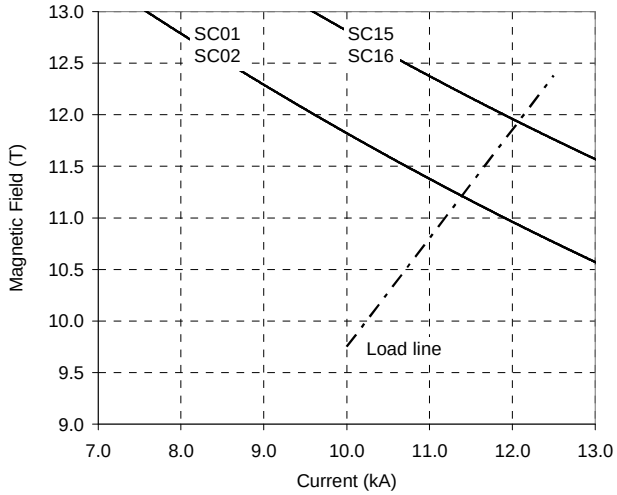

Fig. 2. Measurements of critical current versus magnetic field at 4.5 K for the conductor of coils SC01/SC02 and SC15/SC16 (solid lines), and computed load line for magnet SQ01 (dashed line).

The Lorenz forces in the straight section are directed towards the magnetic mid-plane, in the direction perpendicular to the wide surface of the cable (azimuthal direction), and towards the center of the magnet, in the direction perpendicular to the narrow surface of the cable (radial direction). The required azimuthal and radial pre-stresses are 70 MPa and 5 MPa respectively. Along the longitudinal direction, due to the high energy stored in the magnet, a significant axial force of 96 kN pushes outwardly each coil end, corresponding to an unsupported tension in the straight section of 100 MPa.

III. MECHANICAL DESIGN AND ASSEMBLY

The support structure comprises several components: aluminum bore, stainless steel pads, iron yokes, and aluminum outer shell. As a first step in the assembly, the four coils were placed around the aluminum bore. The functions of the bore are providing an initial alignment structure to position the coils, and supporting the conductors under the action of radial Lorentz forces. The coil-bore assembly was then surrounded by four stainless steel pads, and inserted into a structure composed by a four-piece iron yoke and an aluminum shell. Alignment between the shell and the yokes and between the yokes was ensured by 12 keys.

A 5 mm gap between pads and yokes provided room for inserting four pressurized bladders, which generated the primary force needed to spread the yoke apart, apply tension to the shell and pre-compress the coil-pads subassembly. Once the structure was locked by interference keys, the bladders were deflated and removed. During cool-down, the shell generated further pre-load on the coils, due to the different thermal contractions of aluminum and iron.

In order to reduce the conductor motion in the end region resulting from axial Lorentz forces, a longitudinal support system, similar to the one previously implemented in the HD1 magnet [14], was included in the design (Fig. 3). Four aluminum rods, with a diameter of 25 mm, were inserted in the

four holes of the pads, and bolted to two 50 mm thick stainless steel end plates. The rods were pre-tensioned with an axial piston at room temperature, and, similarly to the outer shell, they significantly increased their stress during cool-down.

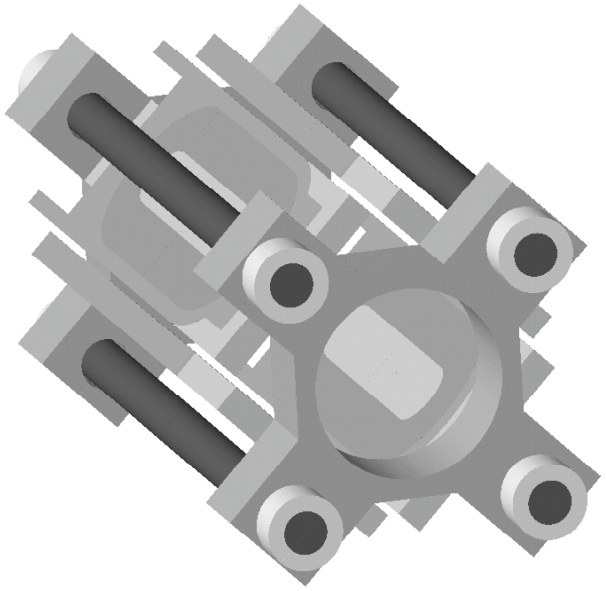

Fig. 3. Longitudinal support: stainless steel end plates and aluminum rods.

The mechanical behavior of the magnet has been analyzed with a 3D finite element model implemented in the code ANSYS, following the same procedure described in [4]. A friction factor $\mu = 0.1$ was assumed between all the surfaces. The results of the computation for the stress in the coil cross-section are depicted in Fig. 4. The graph shows the azimuthal stress in the pole (close to the island) and the mid-plane during assembly, cool-down, and excitation, as a function of the fraction of Lorentz forces with respect to the short sample value $(I/I_{ss})^2$. The pre-stress increases from 21 MPa after the assembly to 85 MPa at 4.5 K. During excitation, the Lorentz forces in the straight section push the conductor towards the mid-plane, unloading the pole. At short sample a stress margin of 20 MPa is predicted by the model.

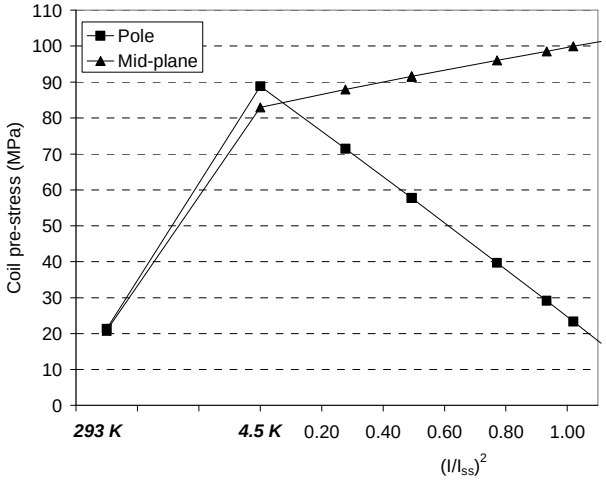

Fig. 4. Computed coil azimuthal pre-stress (MPa) on pole and mid-plane regions during assembly, cool-down and excitation.

IV. Test Results

A. Quench Performance

During the test, 21 training quenches were performed (Fig. 5). The first two quenches occurred at the NbTi-NbTi splice, connecting coils SC01 and SC16. After increasing the LHe level from 60 % to 65 % of the cryostat height, the magnet quenched in coil SC02 at 9.7 kA (85 % of I_{ss}). Since the following two quenches were again located at the splice, the liquid level was further increased to 70 %.

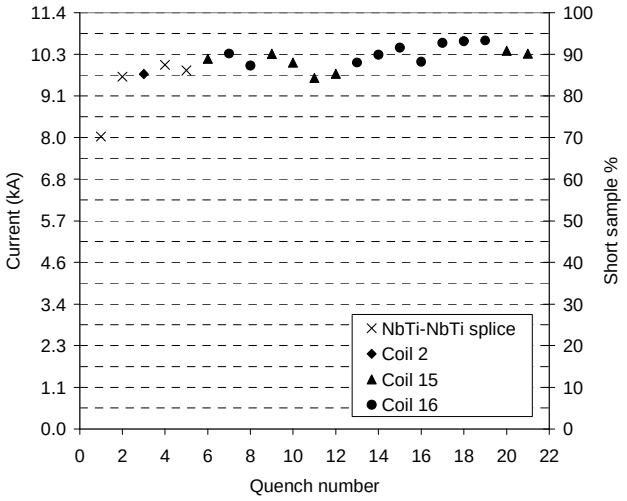

Fig. 5. Current (kA) and short sample percentage of training quenches.

From that point the magnet quenched exclusively in the two new coils (despite a 5 % higher short sample limit with respect to the old coils), reaching a peak current of 10.6 kA (93 % of I_{ss}) on the 19th quench. Analysis of the voltage imbalance indicated that all the quenches were caused by conductor motions (stick-slip).

B. Strain Gauge Measurements

The outer shell has been instrumented with six strain gauges. Four of the gauges (M in Fig. 6) are positioned at the four mid-planes and measure the azimuthal stress. The other two (Z in Fig. 6) measure the shell stress in the longitudinal direction. Four additional strain gauges are attached to the aluminum rods to measure the axial tension. Moreover, full bridge strain gauges were mounted directly over the turns of the new coils and impregnated with them. This technique, which allows measuring the coil's mechanical response during magnet operations, is described in details elsewhere [15]; the results of the coil strain measurements performed on SQ01 will be presented in a future publication. In Fig. 6 we plot the results of the measurements of shell strain performed during assembly, cool-down and excitation, with a comparison to the computed values. With the exception of gauge M01-15, which provides a 25 % lower strain at 4.5 K, three azimuthal gauges measure an average strain variation during cool-down from $500 \cdot 10^{-6}$ (35 MPa of tension) to $1450 \cdot 10^{-6}$ (115 MPa of tension), in close agreement with the computations. Regarding the axial direction, the measured and computed decrease of the strain is mainly due to a Poisson effect, slightly reduced by the friction between the yoke and the shell.

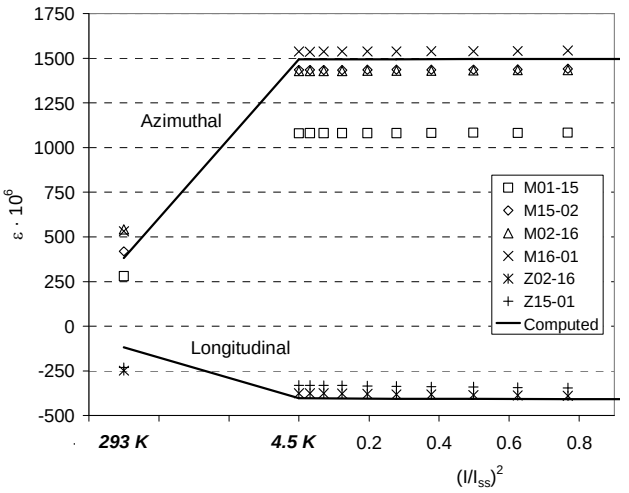

Fig. 6. Azimuthal and longitudinal strain in the shell during assembly, cool-down and excitation: strain gauges measurements (markers) and computations (solid lines).

The strain gauges attached to the rods measure at 4.5 K an average strain of $1950 \cdot 10^{-6}$, corresponding to a tension of 155 MPa. The higher stress computed by the model (190 MPa) may indicate that plastic deformation of one of the axial support components occurred after or during the cool-down.

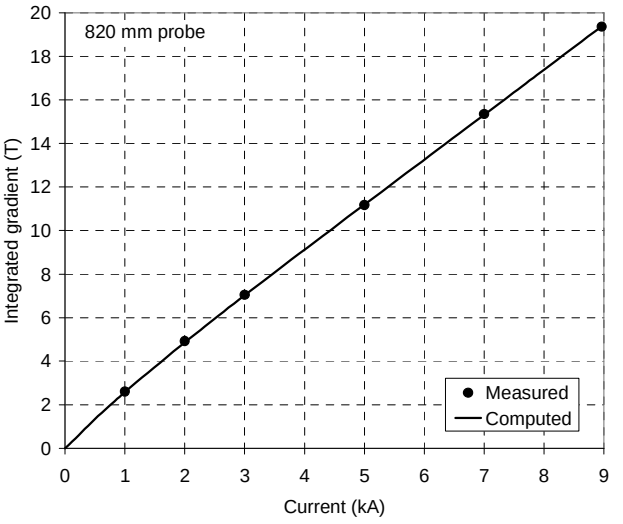

Fig. 7. Integrated gradient (T) at 22 mm radius along a 820 mm probe as a function of the current (kA): field measurements (markers) and computations (solid line).

C. Magnetic Field Measurements

The magnetic field was measured using a rotating coil system. We used a probe 820 mm long and with a diameter of 44.5 mm. The test plan included magnetic measurements at 4.5 K at five different currents. A comparison between the measured and the computed transfer function is given in Fig. 7. The analysis of measured harmonics and their comparison with computations is currently under way.

V. Future Plans

Further investigations of possible causes of training and a retest of the magnet with a different pre-stress configuration will be conducted. In particular, the dependence of performance on coil pre-stress (both radial and longitudinal) and stress limits for Nb_3Sn cables will be studied. Mechanical and thermal response of the coils during excitation and after quenching will be monitored using strain gauges. Furthermore, field quality, correction of magnetic errors, and alignment of magnet components will be addressed.

VI. Conclusions

A Nb_3Sn subscale quadrupole magnet, SQ01, has been designed, fabricated and tested at LBNL. The magnet used racetrack subscale coils developed for the Subscale Magnet Program and arranged for the first time in a quadrupole configuration. SQ01 had a first quench at 85 % of I_{ss} and reached the peak of 93 % of I_{ss} on the 19th quench, producing a gradient of 89 T/m in a 110 mm clear bore. The peak field achieved in the conductor was 10.4 T.

Acknowledgment

We wish to thank Mike Lamm, Clark Reid, Phil Schlabach and Cosmore Sylverster from FNAL for providing a large-diameter rotating probe for magnetic measurements.

References

[1] G. Sabbi, *et al.*, "Nb_3Sn quadrupole magnets for the LHC IR", *IEEE Trans. Appl. Supercond.*, . Vol. 13, no. 2, June 2003, pp. 1262-1265.

[2] A. Zlobin, *et al.*, "Conceptual design study of Nb_3Sn low-beta quadrupole for 2nd generation LHC IRs", *IEEE Trans. Appl. Supercond.*, Vol. 13, no. 2, June 2003, pp. 1266-1269.

[3] R. Gupta, *et al.*, "Next generation IR magnets for hadron colliders", *IEEE Trans. Appl. Supercond.*, Vol. 13, no. 2, June 2003, pp. 1351-1354.

[4] S. Caspi, *et al.*, "Mechanical design of a second generation LHC IR quadrupole", *IEEE Trans. Appl. Supercond.*, Vol. 14, no. 2, June 2004, pp. 235-238.

[5] A. R. Hafalia, *et al.*, "Structure for a 90 mm Nb_3Sn $\cos(2\vartheta)$ IR quadrupole magnet ", this Proceedings.

[6] A. R. Hafalia, *et al.*, "An approach for faster high field magnet technology development", *IEEE Trans. Appl. Superconduct.*, vol. 13, no. 2, June 2003, pp. 1258-1261.

[7] A. R. Hafalia, *et al.*, "A new support structure for high field magnets" *IEEE Trans. Appl. Superconduct.*, vol. 12, no. 1, March 2002, pp. 47.

[8] W. B. Sampson, "Superconducting magnets for beam handling and accelerators", *Proc. 2nd Int. Conf. Magnet Technology* (edited by H. Hadley), Oxford, 1967, pp. 574-578.

[9] A. Asner, C. Becquet, H. Rieder, C. Niqueletto and W. Thomi, "Development and successful testing of the first Nb_3Sn wound, in situ-reacted, high-field superconducting quadrupole of CERN", *IEEE Trans. Magnetics*, vol. MAG-19, no. 3, May 1983, pp. 1410-1416.

[10] N. N. Martovesky, *et al.*, "Development and testing of the improved focusing quadrupole for Heavy Ion Fusion Accelerator", *IEEE Trans. Appl. Superconduct.*, vol. 14, no. 1, June 2004, pp. 316-320.

[11] W. K. McDonald, *et al.*, "Manufacture and evaluation of Nb_3Sn conductors fabricated by the MJR method", *IEEE Trans. Magnetics*, vol. MAG-19, no. 3, May 1983, pp. 1124-1127.

[12] J. A. Parrell, *et al.*, "High field Nb_3Sn conductor development at Oxford Superconducting Technology", *IEEE Trans. Appl. Superconduct.*, vol. 13, no. 2, June 2003, pp. 3470-3473.

[13] D. R. Dietderich, *et al.*, "Correlation between strand stability measurements and magnet performance", this conference.

[14] A. R. Hafalia, *et al.*, "HD1: design and fabrication of a 16 T Nb_3Sn dipole magnet", *IEEE Trans. Appl. Superconduct.*, vol. 14, no. 2, June 2004, pp. 283-286.

[15] S. Caspi, *et al.*, "Measured strain of a Nb_3Sn coil during excitation and quench", this Proceedings.